

Strongly Blue-Shifted C–H Stretches: Interaction of Formaldehyde with Hydrogen Fluoride Clusters

Alfred Karpfen*[†] and Eugene S. Kryachko*[‡]

Institute for Theoretical Chemistry, University of Vienna, Währinger Strasse 17, A-1090 Vienna, Austria, Department of Chemistry, Bat. B6c, University of Liege, Sart-Tilman, B-4000 Liege 1, Belgium, and Bogoliubov Institute for Theoretical Physics, Kiev, 03143 Ukraine

Received: January 24, 2005; In Final Form: June 9, 2005

The equilibrium structures, binding energies, and vibrational spectra of the cyclic, hydrogen-bonded complexes formed between formaldehyde, H₂CO, and hydrogen fluoride clusters, (HF)_{1≤n≤4}, are investigated by means of large-scale second-order Møller–Plesset calculations with extended basis sets. All studied complexes exhibit marked blue shifts of the C–H stretching frequencies, exceeding 100 cm⁻¹ for n = 2–4. It is shown that these blue shifts are, however, only to a minor part caused by blue-shifting hydrogen bonding via C–H···F contacts. The major part arises due to the structural relaxation of the H₂CO molecule under the formation of a strong C=O···H–F hydrogen bond which strengthens as n increases. The close correlation between the different structural parameters in the studied series of complexes is demonstrated, and the consequences for the frequency shifts in the complexes are pointed out, corroborating thus the suggestion of the primary role of the C=O···H–F hydrogen bonding for the C–H stretching frequency shifts. This particular behavior, that the appearance of an increasingly stronger blue shift of the C–H stretching frequencies is mainly induced by the formation of a progressively stronger C=O···H–F hydrogen bond in the series of H₂CO···(HF)_{1≤n≤4} complexes and only to a lesser degree by the formation of the so-called blue-shifting C–H···F hydrogen bond, is rationalized with the aid of selected sections of the intramolecular H₂CO potential energy surface and by performing a variety of structural optimizations of the H₂CO molecule embedded in external, differently oriented dipole electric fields, and also by invoking a simple analytical force-field model.

1. Introduction

Weak hydrogen bonds A–H···X that involve comparatively unpolar proton donor A–H groups, like, e.g., C–H, continue to be the theme of many researchers (see ref 1 for a comprehensive review). The strength of the C–H···X weak hydrogen bonds and their stretching modes $\nu(\text{C–H})$ strongly depends on the nature of the proton donor as C(sp)–H > C(sp²)–H < C(sp³)–H and also increases when hydrogen atoms are successively replaced by electron withdrawing groups (ref 2; see also refs 3 and 1, and ref 4 for current computational studies). Many of the C–H···X hydrogen bonds exhibit peculiar properties such as a contraction of the C–H bond, a blue shift of the C–H stretching vibrational mode, and a decrease of its infrared intensity, which contrast with the well-established features of conventional weak hydrogen bonding.^{1,5–7} Often, these C–H···X hydrogen bonds are termed as blue-shifting hydrogen bonds (see ref 8 for an up-to-date review).

Recent theoretical investigations^{9–11} have demonstrated that the insertion of fluoromethanes or fluorosilanes into hydrogen fluoride rings gives rise to large blue shifts of the C–H or Si–H stretching modes, reaching 50–60 cm⁻¹. The latter are not, however, a direct consequence of the formation of the C–H···F or Si–H···F hydrogen bonds in the fluoromethane···(HF)_{1≤n≤4} or fluorosilane···(HF)_{1≤n≤4} structures, rather they are

to a larger part caused by intramolecular structural relaxations within the fluoromethane and fluorosilane subsystems, which are induced by the formation of considerably stronger C–F···H–F or Si–F···H–F halogen–hydrogen bonds. This has led us to coin these intermolecular C–H···F or Si–H···F contacts as *blue-shifted* hydrogen bonds.^{9,10} The concept of blue-shifting and blue-shifted hydrogen bonds in particular still challenges the researches with many unsolved problems (see, e.g., ref 8) such as, for example, how big is this family of blue-shifting (-shifted) hydrogen bonds and what is the upper limit for a blue shift? The latter two are addressed in the present work.

Herein, we aim to study the interaction of the formaldehyde molecule, H₂CO, with hydrogen fluoride clusters and to provide computational evidence that the C–H stretching vibrational modes are blue-shifted by more than 100 cm⁻¹, when H₂CO is inserted into hydrogen fluoride rings, thereby forming C–H···F and C=O···H–F hydrogen bonds. We also intend to show that the mechanism behind the origin of these large blue shifts has the same roots as those for fluoromethanes···(HF)_{1≤n≤4} or fluorosilanes···(HF)_{1≤n≤4}.^{9–11} Precisely, we demonstrate that the large blue shifts that occur in the H₂CO···HF dimer and in the cyclic H₂CO···(HF)_{2≤n≤4} systems result from the formation of a strong C=O···H–F hydrogen bond that strengthens upon increasing the number of hydrogen fluoride molecules. While the structure and other properties of the dimeric complex H₂CO···HF have already been studied quite extensively, both experimentally^{12,13} as well as theoretically,^{14–20} although without focusing on blue-shifted C–H stretches, the trimeric and higher aggregates have not yet been investigated so far.

* Address correspondence to the authors at the following: Fax +43-1-4277-9527 and e-mail alfred.karpfen@univie.ac.at for A.K. and Fax +32-4-366-3413 and e-mail eugene.kryachko@ulg.ac.be for E.S.K.

[†] University of Vienna.

[‡] University of Liege and Bogoliubov Institute for Theoretical Physics.

2. Computational Methods

All calculations of the complexes $\text{H}_2\text{CO}\cdots(\text{HF})_{1\leq n\leq 4}$ reported in the present work were performed within the second-order perturbation Møller–Plesset frozen-core method (MP2),²¹ using the GAUSSIAN 98 suite of programs.²² Three different basis sets, 6-31+G(d) and 6-311++G(2d,2p),^{23–28} and the extended Dunning-type basis set aug-cc-pVTZ^{29,30} were invoked. Due to the floppy nature of the studied complexes, all geometry optimizations were carried out with the TIGHT option. MP2 harmonic vibrational frequencies were calculated for these complexes to properly characterize stationary points. The effect of the counterpoise (CP) correction³¹ to the basis set superposition error (BSSE) has also been taken into account. Appropriate scans of the potential energy surface (PES) of the H_2CO monomer were performed at the MP2/6-311++G(2d,2p) level. Similar scans with external electric dipole fields (via FIELD option) were performed at the B3LYP/6-311++G(2d,2p) level.

3. Results

Since the properties of $(\text{HF})_n$ clusters have already been amply documented in the literature (see, e.g., Table 2 of ref 9 and refs 32–35), we dispense with a detailed discussion. Some of their properties will, however, be compared with those of the $\text{H}_2\text{CO}\cdots(\text{HF})_{2\leq n\leq 4}$ clusters in Section 4.7.

The formaldehyde molecule H_2CO is the simplest in the class of carbonyl compounds containing the carbonyl group $>\text{C}=\text{O}$, which is the common and most important proton acceptor, for example, in polypeptides and polynucleotides, that participates in hydrogen bond formation in many organic and biological systems.^{1,5–7} This hydrogen bond is formed through a directed lone pair of electrons on the carbonyl oxygen characterized by an sp^2 hybridization (see, e.g., refs 36 and 37). The carbonyl–water hydrogen bond in the case of the formaldehyde–water complex with the interaction energy of about $-5 \text{ kcal}\cdot\text{mol}^{-1}$ is characterized by the H-bond angles $\angle\text{CO}\cdots\text{H}(-\text{OH}) = 101.5^\circ$ and $\angle(\text{H})\text{O}-\text{H}\cdots\text{O}(=\text{C}) = 150.0^\circ$ (CCSD/TZ2P+diff)^{36c} (see also ref 38). Another example worth discussing is the $\text{H}_2\text{CO}-\text{HOCN}$ complex³⁹ where the formed $\text{C}=\text{O}\cdots\text{H}$ hydrogen bond deviates from the $\text{C}=\text{O}$ bond by 135.8° . Interestingly, its formation causes a contraction by 0.003 \AA of the $\text{C}-\text{H}$ bonds of formaldehyde, which is too far remote from the NCOH molecule to exhibit any sort of contact, and a blue shift of the corresponding asymmetric and symmetric $\nu(\text{C}-\text{H})$ stretches by 28 and 43 cm^{-1} , respectively.

The protonation of formaldehyde, a common reaction used to estimate the proton acceptor ability of formaldehyde,⁴⁰ results in a large shortening of its $\text{C}-\text{H}$ bonds (by 0.016 and 0.013 \AA for the MP2/6-311++G(2d,2p) and 0.015 and 0.013 \AA for the MP2/aug-cc-pVTZ) and blue-shifting of its stretches $\nu_{\text{asym}}(\text{C}-\text{H})$ and $\nu_{\text{sym}}(\text{C}-\text{H})$ by 176 and 254 cm^{-1} (MP2/6-311++G(2d,2p)) and 170 and 246 cm^{-1} (MP2/aug-cc-pVTZ), respectively. The comparison of the experimental geometries of the ground-state formaldehyde and protonated formaldehyde⁴¹ shows that the $\text{C}-\text{H}$ bonds are contracted by 0.042 and 0.012 \AA whereas the $\text{C}=\text{O}$ bond is lengthened by 0.040 \AA (in the present work, $\Delta r(\text{C}=\text{O}) = 0.036 \text{ \AA}$ for the MP2/6-311++G(2d,2p) and 0.037 \AA for the MP2/aug-cc-pVTZ). The present calculations estimate the proton affinity of formaldehyde as equal to 168.1 (MP2/6-311++G(2d,2p)) and $167.8 \text{ kcal}\cdot\text{mol}^{-1}$ (MP2/aug-cc-pVTZ), both of which are close to the experimental value of $170.4 \text{ kcal}\cdot\text{mol}^{-1}$.⁴²

The effect of contraction of the $\text{C}-\text{H}$ bonds of formaldehyde under protonation is related to the back-donation of the oxygen lone pair of electrons into the $\text{C}-\text{H}$ bond, precisely, due to the

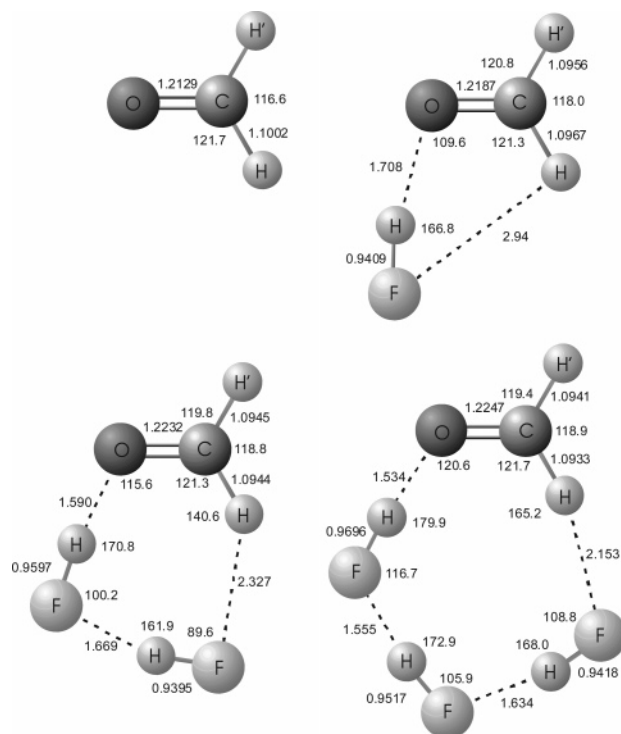


Figure 1. MP2/aug-cc-pVTZ optimized structures of H_2CO and $\text{H}_2\text{CO}\cdots(\text{HF})_{1\leq n\leq 3}$ complexes.

contribution of the trans lone pair to the antibonding $\sigma^*(\text{CH})$ molecular orbital (MO).⁴³ The MO scenario of the protonation of formaldehyde is the following: the added proton is covalently bonded to the carbonyl lone pair and causes a lengthening of the $\text{C}=\text{O}$ bond. This decreases its π character and the dominance of the oxygen atom in the carbon–oxygen interaction (notice that one of the important features of the carbonyl group is the difference in electronegativity between carbon and oxygen that leads to both σ and π electron transfer from C to O and backward, to a positively charged carbon). A protonation causes a substantial charge transfer that is dominated by the charge transfer to C and to the added proton from the formyl protons. The latter are partly destabilized by losing their initial charges, and the $\text{C}-\text{H}$ bonds are therefore shortened.⁴³ The carbon becomes intraatomically stabilized by a gain of charge and the oxygen by the Coulombic attraction to the added proton.

The stable structures of the complexes $\text{H}_2\text{CO}\cdots(\text{HF})_{1\leq n\leq 3}$, optimized within the MP2/aug-cc-pVTZ approach, are sketched in Figure 1. All these complexes have C_s symmetry. The planar structure $\text{H}_2\text{CO}\cdots(\text{HF})_4$ is formally a first-order saddle point. Energetically, it lies in very close vicinity to the minimum energy structure of $\text{H}_2\text{CO}\cdots(\text{HF})_4$, whose H_2CO plane is slightly bent out of the plane of four fluorine atoms (Figure 2). All other internal coordinates of these two $\text{H}_2\text{CO}\cdots(\text{HF})_4$ structures are practically indistinguishable.

The changes in the H_2CO bond lengths induced by the formation of the complexes $\text{H}_2\text{CO}\cdots(\text{HF})_{1\leq n\leq 4}$ are reported in Table 1 invoking all three computational approaches. Table 2 lists the stabilization energies of the studied complexes $\text{H}_2\text{CO}\cdots(\text{HF})_{1\leq n\leq 4}$, viz., ΔE_a , defined relative to H_2CO and $(\text{HF})_n$ rings, and ΔE_b , defined relative to the isolated monomers, H_2CO and $n\text{HF}$, both calculated with and without CP correction to the BSSE. Finally, Tables 3–5 correspondingly report the frequencies of the $\text{C}-\text{H}$, $\text{C}=\text{O}$, and $\text{F}-\text{H}$ stretching vibrational modes, their shifts relative to the corresponding frequencies of the unperturbed monomers, and the associated infrared intensities,

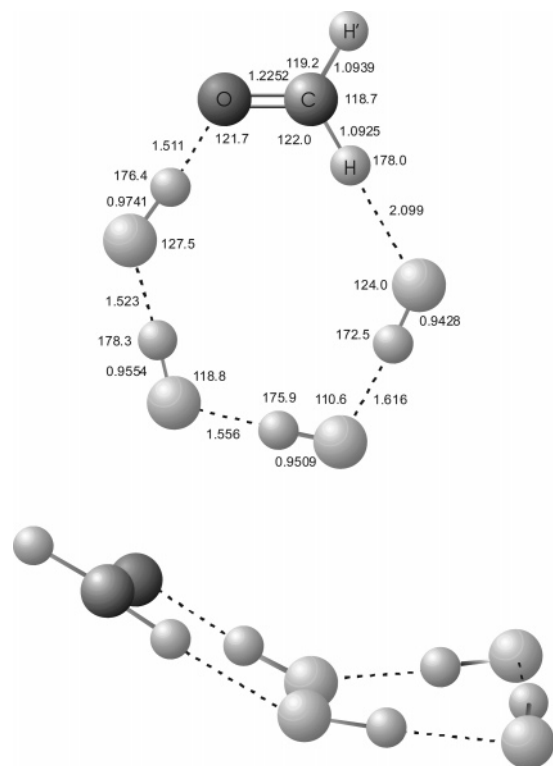


Figure 2. MP2/aug-cc-pVTZ optimized structures of the C_s saddle point (top) and the C_1 minimum (bottom) of the $\text{H}_2\text{CO}\cdots(\text{HF})_4$ complex.

TABLE 1: MP2-Calculated Bond Length Changes in $\text{H}_2\text{CO}-(\text{HF})_n$ Complexes Relative to the H_2CO Monomer (Å)

n	bond length change	basis set		
		6-31+G(d)	6-311++G(2d,2p)	aug-cc-pVTZ
1	$\Delta r(\text{C}-\text{H}')$	-0.0044	-0.0046	-0.0046
	$\Delta r(\text{C}-\text{H})$	-0.0030	-0.0036	-0.0035
	$\Delta r(\text{C}=\text{O})$	0.0052	0.0058	0.0058
2	$\Delta r(\text{C}-\text{H}')$	-0.0052	-0.0057	-0.0057
	$\Delta r(\text{C}-\text{H})$	-0.0057	-0.0062	-0.0058
	$\Delta r(\text{C}=\text{O})$	0.0093	0.0100	0.0103
3	$\Delta r(\text{C}-\text{H}')$	-0.0055	-0.0059	-0.0061
	$\Delta r(\text{C}-\text{H})$	-0.0073	-0.0075	-0.0069
	$\Delta r(\text{C}=\text{O})$	0.0106	0.0113	0.0118
4 ^a	$\Delta r(\text{C}-\text{H}')$	-0.0057	-0.0061	-0.0063
	$\Delta r(\text{C}-\text{H})$	-0.0080	-0.0082	-0.0077
	$\Delta r(\text{C}=\text{O})$	0.0109	0.0116	0.0123
4 ^b	$\Delta r(\text{C}-\text{H}')$	-0.0073	-0.0063	-0.0066
	$\Delta r(\text{C}-\text{H})$	-0.0084	-0.0082	-0.0079
	$\Delta r(\text{C}=\text{O})$	0.0093	0.0119	0.0126

^a C_s saddle point. ^b C_1 minimum.

obtained within the MP2/6-311++G(2d,2p) and MP2/aug-cc-pVTZ approaches.

4. Discussion

4.1. The Dimer $\text{H}_2\text{CO}\cdots\text{HF}$. The interaction of hydrogen fluoride with formaldehyde leads to a very stable dimeric complex with the stabilization energy $\Delta E_a^{(1)} = \Delta E_b^{(1)} \approx -8$ kcal·mol⁻¹, indicative of a very strong F-H \cdots O=C hydrogen bond. On the other hand, the distance of about 2.94 Å between the F atom and the nearest hydrogen atom H of formaldehyde is somewhat larger than the sum of the van der Waals radii of F and H (~ 2.90 Å), hence their contact C-H \cdots F cannot be firmly characterized as a “hydrogen bond”.^{5,6} Nevertheless, despite the absence of a C-H \cdots F hydrogen bond in $\text{H}_2\text{CO}\cdots\text{HF}$, both C-H bonds undergo substantial changes relative to

TABLE 2: MP2-Calculated Stabilization Energies of $\text{H}_2\text{CO}-(\text{HF})_n$ Complexes (kcal·mol⁻¹)

n		basis set		
		6-31+G(d)	6-311++G(2d,2p)	aug-cc-pVTZ
1	$\Delta E_{a,b}$	-9.0 (-7.4) ^a	-8.4 (-7.2)	-8.6 (-7.9)
2	ΔE_a	-13.8 (-11.8)	-13.5 (-11.4)	-13.8 (-12.8)
	ΔE_b	-19.4 (-16.1)	-18.1 (-15.2)	-18.5 (-15.9)
3	ΔE_a	-13.0 (-10.7)	-12.2 (-10.1)	-13.0 (-11.8)
	ΔE_b	-30.3 (-25.1)	-27.8 (-23.1)	-28.4 (-25.9)
4 ^b	ΔE_a	-8.7 (-6.3)	-8.4 (-6.4)	-8.4
	ΔE_b	-40.2 (-33.2)	-36.6 (-30.4)	-37.4
4 ^c	ΔE_a	-9.6 (-6.9)	-8.5 (-6.4)	-8.6
	ΔE_b	-41.1 (-33.8)	-36.7 (-30.5)	-37.6

^a Counterpoise-corrected energies in parentheses. ^b C_s saddle point. ^c C_1 minimum.

TABLE 3: Selected MP2-Calculated Harmonic Vibrational Frequencies of the H_2CO and HF Monomer Stretching Modes (cm⁻¹) and Their Infrared Intensities (km·mol⁻¹)

		basis set	
		6-311++G(2d,2p)	aug-cc-pVTZ
H_2CO	$\nu(\text{C}=\text{O})$	1747 (67) ^a	1753 (68)
	$\nu(\text{C}-\text{H})$, sym	2971 (68)	2973 (67)
	$\nu(\text{C}-\text{H})$, asym	3048 (97)	3047 (88)
HF	$\nu(\text{F}-\text{H})$	4164 (127)	4124 (121)

^a Infrared intensities in parentheses.

TABLE 4: Selected MP2-Calculated Harmonic Vibrational Frequencies of $\text{H}_2\text{CO}-(\text{HF})_n$ ($n=1-3$) Complexes, Their Frequency Shifts Relative to Monomers (cm⁻¹), and Their Infrared Intensities (km·mol⁻¹)

n		basis set ^{a,b}	
		6-311++G(2d,2p)	aug-cc-pVTZ
1	$\nu(\text{C}=\text{O})$	1735 (-12) [69]	1740 (-13) [71]
	$\nu(\text{C}-\text{H})$, sym	3016 (45) [47]	3017 (44) [46]
	$\nu(\text{C}-\text{H})$, asym	3115 (67) [43]	3115 (68) [39]
2	$\nu(\text{F}-\text{H})$	3778 (-386) [907]	3693 (-431) [946]
	$\nu(\text{C}=\text{O})$	1724 (-23) [69]	1728 (-25) [72]
	$\nu(\text{C}-\text{H})$, sym	3036 (65) [66]	3036 (63) [77]
3	$\nu(\text{C}-\text{H})$, asym	3150 (102) [13]	3148 (101) [12]
	$\nu(\text{F}-\text{H})$	3440 (-724) [1351]	3325 (-799) [1397]
	$\nu(\text{F}-\text{H})$	3855 (-309) [599]	3763 (-361) [645]
3	$\nu(\text{C}=\text{O})$	1726 (-21) [85]	1728 (-25) [93]
	$\nu(\text{C}-\text{H})$, sym	3036 (65) [112]	3040 (67) [317]
	$\nu(\text{C}-\text{H})$, asym	3167 (119) [10]	3165 (118) [19]
	$\nu(\text{F}-\text{H})$	3277 (-887) [1852]	3118 (-1004) [1784]
	$\nu(\text{F}-\text{H})$	3658 (-506) [934]	3525 (-597) [1041]
	$\nu(\text{F}-\text{H})$	3832 (-332) [684]	3726 (-396) [724]

^a Frequency shifts in parentheses. ^b Infrared intensities in square brackets.

the isolated H_2CO molecule. It is definitely the formation of the F-H \cdots O=C hydrogen bond that contracts both C-H bonds by ca. -0.004 Å and simultaneously elongates the C=O bond by about 0.006 Å. Interestingly, the more remote C-H' group is contracted somewhat stronger. These structural distortions significantly modify the C-H and C=O stretching modes of the dimer. More specifically, the symmetric and asymmetric C-H stretching modes are calculated to be blue-shifted by 44 and 68 cm⁻¹, respectively (MP2/aug-cc-pVTZ). The C=O stretching mode undergoes a small downshift, while the F-H stretching mode is strongly red-shifted. The infrared intensities of both $\nu(\text{C}-\text{H})$ are significantly lowered, that of the $\nu(\text{C}=\text{O})$ mode remains almost unchanged, whereas the intensity of $\nu(\text{F}-\text{H})$ is strongly enhanced. This pattern, typical of blue-shifted X-H \cdots F hydrogen bonds, even without actually forming a hydrogen bond, has also been encountered for the dimeric

TABLE 5: Selected MP2/6-311++G(2d,2p)-Calculated Harmonic Vibrational Frequencies of the $\text{H}_2\text{CO}-(\text{HF})_4$ Complex, Their Frequency Shifts Relative to Monomers (cm^{-1}), and Their Infrared Intensities ($\text{km}\cdot\text{mol}^{-1}$)

	C_s saddle ^{a,b}	C_1 minimum ^{a,b}
$\nu(\text{C}=\text{O})$	1729 (-18) [96]	1726 (-21) [94]
$\nu(\text{C}-\text{H})$, sym	3048 (77) [160]	3048 (77) [201]
$\nu(\text{C}-\text{H})$, asym	3176 (128) [56]	3175 (127) [659]
$\nu(\text{F}-\text{H})$	3211 (-953) [2174]	3184 (-980) [1521]
$\nu(\text{F}-\text{H})$	3585 (-579) [1303]	3562 (-602) [1153]
$\nu(\text{F}-\text{H})$	3707 (-457) [852]	3696 (-468) [920]
$\nu(\text{F}-\text{H})$	3823 (-341) [640]	3824 (-340) [668]

^a Frequency shifts in parentheses. ^b Infrared intensities in square brackets.

complexes of HF with the fluoromethanes CH_3F and CH_2F_2 ,¹⁰ and with the three fluorosilanes SiHF_3 , SiH_2F_2 , and SiH_3F .¹¹

4.2. The Complexes $\text{H}_2\text{CO}\cdots(\text{HF})_n$, $n = 2, 3$. These complexes are cyclic, with planar, C_s -symmetric equilibrium structures. In addition to the strong, conventional and red-shifted hydrogen bonds $\text{F}-\text{H}\cdots\text{O}=\text{C}$ and $\text{F}-\text{H}\cdots\text{F}$, a $\text{C}-\text{H}\cdots\text{F}$ contact is now also formed in $\text{H}_2\text{CO}\cdots(\text{HF})_n$ ($n = 2, 3$). Since $R(\text{H}\cdots\text{F}) = 2.33 \text{ \AA}$ for $n = 2$ and 2.15 \AA for $n = 3$, these $\text{C}-\text{H}\cdots\text{F}$ contacts are sufficiently short (see Figure 1) to be treated as hydrogen bonds.^{5,6} Both complexes are strongly bound relative to H_2CO and the well-known C_s minimum of $(\text{HF})_2$ ($\Delta E_a^{(2)} = -12.8 \text{ kcal}\cdot\text{mol}^{-1}$) and cyclic $(\text{HF})_3$ ($\Delta E_a^{(3)} = -11.8 \text{ kcal}\cdot\text{mol}^{-1}$).

Both $\text{C}-\text{H}$ bonds are stronger contracted whereas the $\text{C}=\text{O}$ bond is more elongated as the ring size increases. Relative to the monomer, the $\text{C}-\text{H}$ blue shifts become considerably large and amount to the following: (i) $n = 2$, 63 cm^{-1} for the lower lying symmetric $\text{C}-\text{H}$ stretch and 101 cm^{-1} for the higher lying asymmetric; (ii) $n = 3$, 67 cm^{-1} for the symmetric and 118 cm^{-1} for the asymmetric $\text{C}-\text{H}$ stretch (MP2/aug-cc-pVTZ). These are, to our knowledge, the largest theoretical blue shifts obtained so far for $\text{C}-\text{H}\cdots\text{F}$ hydrogen bonds. It is worth mentioning that compared to the dimer, the infrared intensity of the symmetric $\text{C}-\text{H}$ stretch increases in $\text{H}_2\text{CO}\cdots(\text{HF})_2$, whereas that of the asymmetric one further decreases. Due to a partial mixing with lower lying $\text{F}-\text{H}$ stretching modes in the complex $\text{H}_2\text{CO}\cdots(\text{HF})_3$, a lower intensity is calculated only for the asymmetric $\text{C}-\text{H}$ stretch while that of the symmetric stretch is strongly enhanced.

4.3. The Complex $\text{H}_2\text{CO}\cdots(\text{HF})_4$. This pentameric cluster is still distinctly stable with respect to dissociation to H_2CO and cyclic $(\text{HF})_4$. The CP-corrected stabilization energy $\Delta E_a^{(4)}$ of $-6.4 \text{ kcal}\cdot\text{mol}^{-1}$ is, however, smaller, by the absolute value, than the $\Delta E_a^{(2)}$ and $\Delta E_a^{(3)}$ values, a mere consequence of the well-known high stability of cyclic $(\text{HF})_4$. All the structural and vibrational spectroscopic trends observed so far for the cases $n = 1-3$ are also encountered for $n = 4$. All intermolecular contacts are now shorter. Even the $\text{C}-\text{H}\cdots\text{F}$ contact, characterized by $R(\text{H}\cdots\text{F}) = 2.1 \text{ \AA}$, is shortened. The contractions of the $\text{C}-\text{H}$ bonds in the C_s structure and in the energetically closer lying C_1 minimum are nearly identical (-0.0063 and -0.0077 \AA vs -0.0066 and -0.0079 \AA , respectively; MP2/aug-cc-pVTZ). The blue shifts calculated within the MP2/6-311++G-(2d,2p) approach appear to be even larger, viz., 77 and 127 cm^{-1} for symmetric and asymmetric $\text{C}-\text{H}$ stretches, respectively. The $\text{C}-\text{H}$ stretching modes are strongly mixed in $\text{H}_2\text{CO}\cdots(\text{HF})_4$ with the lower lying $\text{F}-\text{H}$ stretchings. Hence, the typical reduction of the infrared intensities is no longer observable.

4.4. Some Correlations in the Series $\text{H}_2\text{CO}\cdots(\text{HF})_{1\leq n\leq 4}$. As anticipated, most of the structural properties of the studied

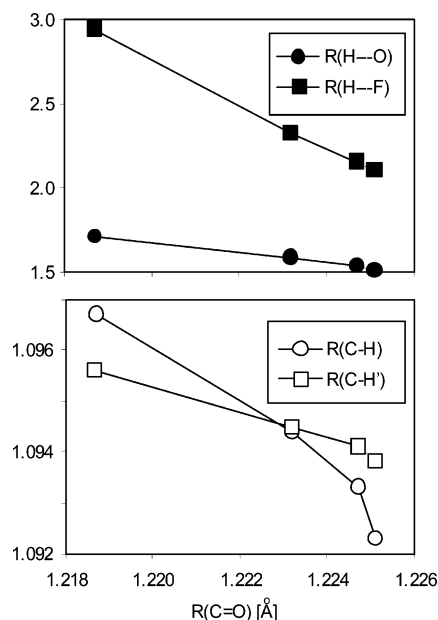


Figure 3. Correlation between the MP2/aug-cc-pVTZ optimized $\text{C}=\text{O}$ distance and other optimized bond distances in the series of $\text{H}_2\text{CO}\cdots(\text{HF})_{1\leq n\leq 4}$ complexes.

$\text{H}_2\text{CO}\cdots(\text{HF})_{1\leq n\leq 4}$ complexes are fairly correlated. Since the correlations between $R(\text{C}=\text{O})$, on one hand, and $R(\text{C}-\text{H})$ and $R(\text{C}-\text{H}')$, on the other, are discussed above for the dimeric complex $\text{H}_2\text{CO}\cdots\text{HF}$, $R(\text{C}=\text{O})$ is further chosen as a reference bond length to extend these correlations for the whole series $\text{H}_2\text{CO}\cdots(\text{HF})_{2\leq n\leq 4}$. In Figure 3, we display the two optimized intermolecular distances $R(\text{H}\cdots\text{O})$ and $R(\text{H}\cdots\text{F})$ (the upper panel) and the optimized distances $R(\text{C}-\text{H})$ and $R(\text{C}-\text{H}')$ (the lower panel) as functions of $R(\text{C}=\text{O})$ for the whole studied series $\text{H}_2\text{CO}\cdots(\text{HF})_{1\leq n\leq 4}$. Inspecting this figure, we conclude that all four correlations are very smooth, indeed, most of them are even linear. Within this series, the $\text{C}=\text{O}$ distance gradually increases as a result of the formation of $\text{F}-\text{H}\cdots\text{O}=\text{C}$ hydrogen bonds of increasing strengths. Both $\text{H}\cdots\text{O}$ and $\text{H}\cdots\text{F}$ intermolecular contacts are contracted and so are the $\text{C}-\text{H}$ bonds of the H_2CO molecule. We assume that the latter intramolecular correlation definitely originates from the internal structure of the H_2CO and its force field in particular. This viewpoint is discussed in the next section.

4.5. Intramolecular PES of H_2CO . By analogy with the previous studies of fluoromethanes $\cdots(\text{HF})_{1\leq n\leq 4}$ and fluorosilanes $\cdots(\text{HF})_{1\leq n\leq 4}$ systems,⁹⁻¹¹ we postulate that the specific structural response of the H_2CO molecule to the $(\text{HF})_{1\leq n\leq 4}$ rings is mostly determined by its intramolecular force field. A rather convenient way to prove this hypothesis is to show the appropriate sections of the PES of H_2CO (the complete MP2/6-311++G(2d,2p) optimization of all the remaining geometrical parameters is implied), viz., (a) Sections 1 and 2: $R(\text{C}-\text{H}')$ and $R(\text{C}=\text{O})$ as functions of $R(\text{C}-\text{H})$ (the upper panels of Figure 4); (b) Sections 3 and 4: $R(\text{C}-\text{H})$ and the bond angle $\angle\text{HCH}'$ as functions of $R(\text{C}=\text{O})$ (the lower panels of Figure 4).

The third section (scan of $R(\text{C}=\text{O})$ and optimization of $R(\text{C}-\text{H})$) of the PES of H_2CO can also be interpreted in terms of a simplified analytical harmonic force-field model. Within the harmonic approximation, the potential energy of H_2CO in the vicinity of its equilibrium geometry is represented by

$$U^h(R, r, r') = (1/2)F_{11}S_1^2 + F_{12}(S_1S_2 + S_1S_3) + (1/2)F_{22}(S_2^2 + S_3^2) + F_{23}S_2S_3 \quad (1)$$

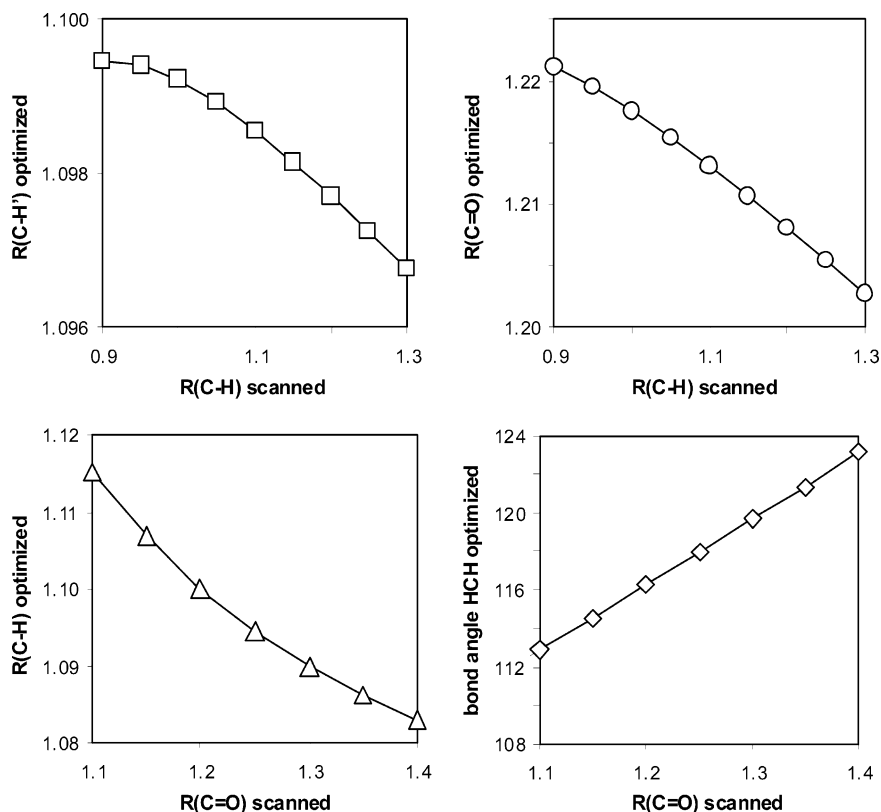


Figure 4. Selected intramolecular sections of the H₂CO PES as obtained at the MP2/6-311++G(2d,2p) level. All values are given in Å.

where $R \equiv R(\text{C}=\text{O})$, $r \equiv R(\text{C}-\text{H})$, $r' \equiv R(\text{C}-\text{H}')$, $S_1 \equiv (R - R_e)/R_e$, $S_2 \equiv (r - r_e)/r_e$, $S_3 \equiv (r' - r'_e)/r'_e$, and the subscript “e” stands for the equilibrium (see, e.g., ref 44). Obviously, the form of eq 1 suggests that the changes in the bond angle $\angle\text{HCH}'$ and its coupling with the bond-lengths degrees of freedom are henceforth neglected. To make use of the C_{2v} symmetric equilibrium structure of H₂CO, we define the symmetry-adapted relative stretching displacements $Q_{23} \equiv (S_2 + S_3)/2$ and $q_{23} \equiv S_2 - S_3$, and rewrite $U^{\text{h}}(R, r, r')$ as

$$U_{\text{sym}}^{\text{h}}(R, Q_{23}, q_{23}) = (1/2)F_{11}S_1^2 + 2F_{12}S_1Q_{23} + (F_{22} + F_{23})Q_{23}^2 + (1/4)(F_{22} - F_{23})q_{23}^2 \quad (2)$$

Let us consider the C=O bond as a “spectator” bond fixed at some length R_0 that corresponds to $S_1^o \equiv (R_0 - R_e)/R_e$. $U_{\text{sym}}^{\text{h}}(R, Q_{23}, q_{23})$ becomes then a function

$$u_{\text{sym}}^{\text{h}}(Q_{23}; R_0) = 2F_{12}S_1^oQ_{23} + (F_{22} + F_{23})Q_{23}^2 \quad (3)$$

of Q_{23} that parametrically depends on R_0 through S_1^o . Notice that the last term on the right-hand side of eq 2 is removed as decoupled from S_1 . An extremum of $u_{\text{sym}}^{\text{h}}(Q_{23}; R_0)$ is attained at $Q_{23}^{o\text{h}}$ as function of S_1^o that obeys the following linear algebraic equation:

$$F_{12}S_1^o + (F_{22} + F_{23})Q_{23}^{o\text{h}} = 0 \quad (4)$$

Therefore,

$$Q_{23}^{o\text{h}} = -[F_{12}/(F_{22} + F_{23})]S_1^o \equiv \alpha_{\text{h}}S_1^o \quad (5)$$

where α_{h} is a so-called harmonic response factor. Substituting the values of the harmonic force constants $F_{12} = 0.714$ aJ, $F_{22} = 2.964$ aJ, and $F_{23} = 0.086$ aJ reported in ref 44

into eq 5 yields its magnitude

$$\alpha_{\text{h}} = -0.234 \quad (6)$$

Therefore, since the ratio $Q_{23}^{o\text{h}}/S_1^o$ is negative or, equivalently, the harmonic response factor is negative, an elongation of the spectator C=O bond causes a contraction of the C–H bonds. Obviously, the negative sign of the harmonic response factor is completely determined by the sign of the intramolecular coupling F_{12} .

An inclusion of first-order anharmonic corrections converts the harmonic potential (3) into the following

$$u_{\text{sym}}^{\text{anh}}(Q_{23}; R_0) = 2F_{12}S_1^oQ_{23} + (F_{22} + F_{23})Q_{23}^2 + (1/6)F_{112}(S_1^o)^2Q_{23} + (1/3)F_{222}Q_{23}^3 \quad (7)$$

For a given length S_1^o of the spectator C=O bond, the latter has an extremum determined to the second order of S_1^o by the following expression

$$Q_{23}^{o\text{anh}} = \alpha_{\text{h}}S_1^o - \{(2F_{222}\alpha_{\text{h}}^2 + F_{112})/[12(F_{22} + F_{23})]\}(S_1^o)^2 \quad (8)$$

Since the anharmonic force constants $F_{112} = -1.009$ aJ and $F_{222} = -0.876$ aJ [ref 44] are both negative, the second term in the right-hand side of eq 8 is positive and equal to $0.030(S_1^o)^2$. This means that the first-order anharmonic corrections only slightly weaken the negative response provided by the harmonic intramolecular coupling constant. For instance, for a given $S_1^o = 0.2$, we obtain $Q_{23}^{o\text{h}} \approx -0.047$ and $Q_{23}^{o\text{anh}} \approx -0.046$, that is, the relative weakening of the negative response due to the first-order anharmonic corrections amounts to only $|Q_{23}^{o\text{h}} - Q_{23}^{o\text{anh}}|/|Q_{23}^{o\text{h}}| \approx 2.6\%$, and therefore can be simply neglected.

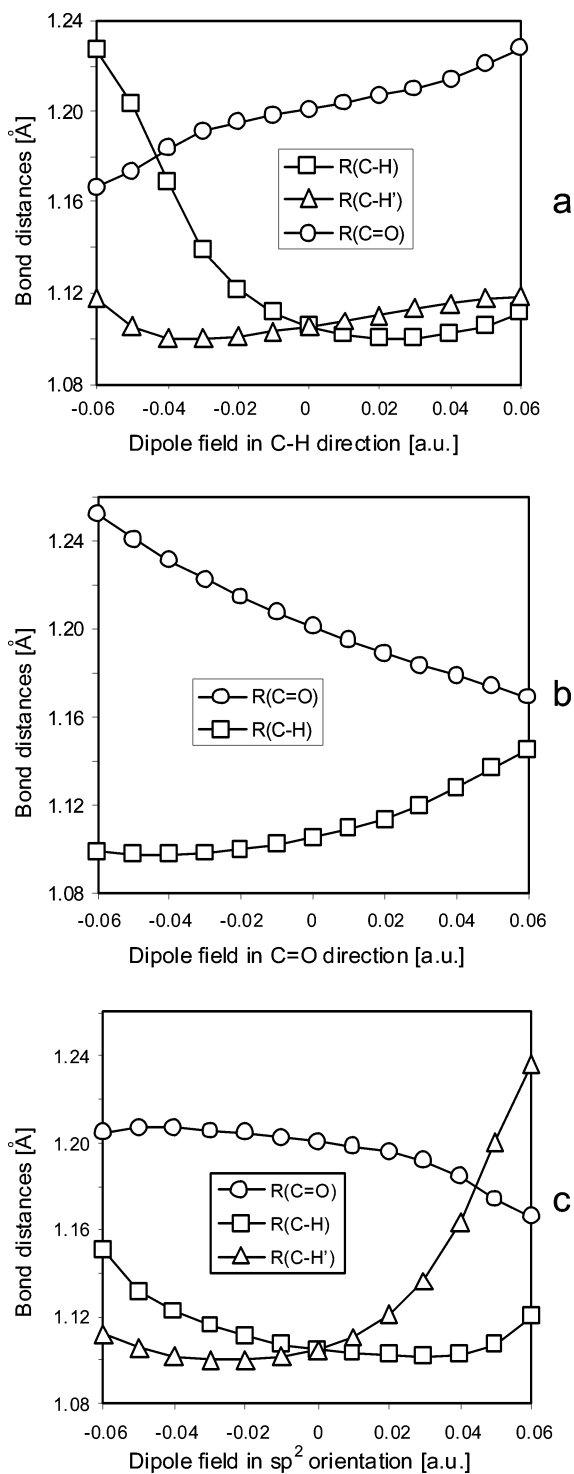


Figure 5. Geometry relaxation of the H_2CO molecule in external homogeneous dipole fields as obtained at the B3LYP/6-311++G(2d,-2p) level.

This simple analytical model demonstrates that $R(\text{C}=\text{O})$ and $R(\text{C}-\text{H})$ are inversely coupled. The following conclusions can be readily drawn from Figure 4: (i) if one of the $\text{C}-\text{H}$ bonds is stretched, the other one is contracted along with the $\text{C}=\text{O}$ bond; (ii) an elongation of the $\text{C}=\text{O}$ bond significantly shortens $R(\text{C}-\text{H})$. That agrees with the analytical model. These findings are consistent with what we observe above in the complexes $\text{H}_2\text{CO}\cdots(\text{HF})_{1\leq n\leq 4}$, where the formation of the strong $\text{C}=\text{O}\cdots\text{H}-\text{F}$ hydrogen bond triggers the elongation of the $\text{C}=\text{O}$ bond. The latter causes a contraction of the $\text{C}-\text{H}$ and $\text{C}-\text{H}'$ bonds

and as a consequence, the $\text{C}-\text{H}$ and $\text{C}-\text{H}'$ stretching vibrational modes experience blue shifts.

4.6. Effect of External Electric Dipole Field on PES of Formaldehyde. The structural response of the H_2CO molecule to a relatively weak external electric dipole field is also governed by its intramolecular PES. In this regard, it is worth mentioning that the influence of an electric dipole field on the $\text{C}-\text{H}$ bonds has already been discussed in the literature.⁴⁵⁻⁴⁷

Figure 5 displays the results of the complete B3LYP/6-311++G(2d,2p) geometry optimizations of the H_2CO molecule embedded into an external electric dipole field that is either oriented along one of the $\text{C}-\text{H}$ bonds (Figure 5a), or along the $\text{C}=\text{O}$ bond (Figure 5b), or along the HF molecule in the $\text{H}_2\text{CO}\cdots\text{HF}$ dimer, i.e., approximately along the direction of the sp^2 lone pair of the oxygen atom (Figure 5c). The total energy of the dimer is lowered only for a positive electric field applied along the $\text{C}-\text{H}$ bond and/or for a negative one in the other cases. In the former case shown in Figure 5a, a weak electric field causes a contraction of the $\text{C}-\text{H}$ bond and simultaneous elongations of the $\text{C}-\text{H}'$ and $\text{C}=\text{O}$ bonds. This $\text{C}-\text{H}$ contraction is a typical feature of $\text{X}-\text{H}$ bonds that exhibit blue shifts upon hydrogen bonding interaction. The elongations that $\text{C}-\text{H}'$ and $\text{C}=\text{O}$ undergo are mostly attributed to the intramolecular couplings discussed in the previous section. On the other hand, the negative field applied parallel to the $\text{C}=\text{O}$ bond contracts the $\text{C}-\text{H}$ bond and stretches the $\text{C}=\text{O}$ bond (see Figure 5b), in complete agreement with the PES sections discussed above.

In the $\text{H}_2\text{CO}\cdots\text{HF}$ dimer and also in the larger $\text{H}_2\text{CO}\cdots(\text{HF})_n$ rings, the HF molecule that participates in the $\text{F}-\text{H}\cdots\text{O}=\text{C}$ hydrogen bond is oriented approximately in the direction of one of the oxygen lone pairs. This makes Figure 5c rather instructive for our purpose as though it reveals some limitations of such a simplified model of an external homogeneous electric field. In this sp^2 orientation, $R(\text{C}=\text{O})$ is again elongated for negative field strength (attractive energy), whereas $R(\text{C}-\text{H}')$, the more distant $\text{C}-\text{H}$ distance, contracts. However, $R(\text{C}-\text{H})$ is now also elongated, reflecting the fact that the orientation of $R(\text{C}-\text{H})$ relative to the field is very different from that in Figure 5a.

The harmonic force-field model (1) can be generalized to include a weak external field:

$$U^{\text{h field}}(R, r, r') = (1/2)F_{11}S_1^2 + F_{12}(S_1S_2 + S_1S_3) + (1/2)F_{22}(S_2^2 + S_3^2) + F_{23}S_2S_3 - (\beta_1E_1S_1 + \beta_2E_2S_2 + \beta_3E_3S_3) \quad (9)$$

where $\beta_i = q_i r_{ie} \cos \varphi_i$, φ_i is the angle between an external field \mathbf{E}_i and the i th bond dipole moment $\mathbf{d}_i = q_i \mathbf{r}_i$ ($i = 1-3$), and $r_1 = R(\text{C}=\text{O})$, $r_2 = R(\text{C}-\text{H})$, $r_3 = R(\text{C}-\text{H}')$. We only consider below a particular case of eq 9 when the carbonyl bond length is fixed at R^o that determines the relative value of S_1^o . As a result, eq 9 recasts as

$$u^{\text{h field}}(S_2, S_3; R^o) = F_{12}S_1^o(S_2 + S_3) + (1/2)F_{22}(S_2^2 + S_3^2) + F_{23}S_2S_3 - (\beta_2E_2S_2 + \beta_3E_3S_3) \quad (10)$$

$u^{\text{h field}}(S_2, S_3; R^o)$ has the extremum at S_2^o and S_3^o satisfying the following pair of algebraic equations

$$\begin{aligned} F_{22}S_2^o + F_{23}S_3^o &= -F_{12}S_1^o + \beta_2E_2 \\ F_{23}S_2^o + F_{22}S_3^o &= -F_{12}S_1^o + \beta_3E_3 \end{aligned} \quad (11)$$

The solution of eq 11 is straightforward, viz.,

$$S_2^o = \alpha_h S_1^o + (\beta_2 E_2 F_{22} - \beta_3 E_3 F_{23}) / \Delta$$

$$S_3^o = \alpha_h S_1^o + (\beta_3 E_3 F_{22} - \beta_2 E_2 F_{23}) / \Delta \quad (12)$$

where $\Delta = F_{22}^2 - F_{23}^2$. In the absence of an external electric field, eq 12 is transformed into eq 5.

Let us assume that an external electric field is homogeneous. This considerably simplifies eq 12:

$$S_2^o = S_3^o = \alpha_h S_1^o + \beta E / (F_{22} + F_{23}) \quad (13)$$

where $\beta_2 = \beta_3 = \beta$. Therefore, if β is positive, the negative electric field causes additional contraction of both the C–H bonds of H_2CO . If the electric field is positive, there exists a threshold value $E_{\text{thr}} = \alpha_h (F_{22} + F_{23}) / \beta = F_{12} / \beta$ such that in the case of $E < E_{\text{thr}}$, the C–H bonds are less contracted than without a field. If $E > E_{\text{thr}}$, the positive electric field leads to elongation of the C–H bonds.

4.7. Hydrogen Bond Cooperativity in $\text{H}_2\text{CO}\cdots(\text{HF})_{1\leq n\leq 4}$ Clusters. Small hydrogen fluoride rings $(\text{HF})_n$ are among the best investigated hydrogen-bonded clusters. For more detailed reviews of their structural, energetic, and vibrational spectroscopic properties see refs 32–35. Cooperative or nonadditive effects of intermolecular interaction, dominated by polarization nonadditivities, lead to substantial increases of stabilization energies, considerable shortenings of intermolecular F(H) \cdots F contacts, and significant elongations of intramolecular H–F distances. These structural distortions are accompanied by large red shifts of H–F stretching frequencies gradually approaching the 920 cm^{-1} difference between the isolated HF molecule and the anisotropic molecular solid HF and also by large increases of the frequencies of the intermolecular modes into a region close to 1000 cm^{-1} .

In this section, we intend to explain and discuss some of the trends in the $(\text{HF})_n$ moieties of the $\text{H}_2\text{CO}\cdots(\text{HF})_{2\leq n\leq 4}$ clusters by comparing them to the series of $(\text{HF})_n$ rings. The most obvious way to proceed is to consider the $\text{H}_2\text{CO}\cdots(\text{HF})_{2\leq n\leq 4}$ cluster as originating from an $(\text{HF})_{n+1}$ ring where one HF molecule is replaced by an H_2CO molecule. In the C_{nh} -symmetric $(\text{HF})_3$, $(\text{HF})_4$, and $(\text{HF})_5$ rings, the bond angles F–H \cdots F are calculated (MP2/aug-cc-pVTZ) as 147.2° , 164.9° , and 174.2° , respectively, thus forming more linear hydrogen bonds with increasing ring size. The F–H \cdots F bond angles (see Figures 1 and 2) in $\text{H}_2\text{CO}\cdots(\text{HF})_2$ (161.9°), $\text{H}_2\text{CO}\cdots(\text{HF})_3$ (172.9° , 168.0°), and $\text{H}_2\text{CO}\cdots(\text{HF})_4$ (172.5° , 175.9° , and 178.3°) show precisely the same trend. The gradual contraction of the intermolecular H \cdots F distances in the series $(\text{HF})_3$, $(\text{HF})_4$, and $(\text{HF})_5$ (1.769, 1.583, and 1.528 \AA) is also found in the $\text{H}_2\text{CO}\cdots(\text{HF})_{2\leq n\leq 4}$ series: 1.669 \AA ($n = 2$), 1.634 and 1.555 \AA ($n = 3$), and 1.523 , 1.556 , and 1.616 \AA ($n = 4$). The same applies to the systematic increase of intramolecular HF distances: on one hand, $r(\text{F–H}) = 0.9218$, 0.9392 , 0.9520 , and 0.9568 \AA in HF monomer, $(\text{HF})_3$, $(\text{HF})_4$, and $(\text{HF})_5$, and, on the other, 0.9395 \AA in $\text{H}_2\text{CO}\cdots(\text{HF})_2$, 0.9418 and 0.9517 \AA in $\text{H}_2\text{CO}\cdots(\text{HF})_3$, and 0.9428 , 0.9509 , and 0.9554 \AA in $\text{H}_2\text{CO}\cdots(\text{HF})_4$. In parallel, the corresponding HF stretching frequencies are strongly red-shifted. Relative to the HF monomer with the harmonic $\nu(\text{F–H}) = 4124\text{ cm}^{-1}$ (MP2/aug-cc-pVTZ, Table 3) stretching frequency, the calculated red shifts amount to -413 and -292 (d) cm^{-1} for $(\text{HF})_3$, -779 , -568 (d), and -486 cm^{-1} for $(\text{HF})_4$ and -927 , -707 (d), and -579 cm^{-1} for $(\text{HF})_5$, where (d) indicates the doubly degenerate, infrared-active modes. Incorporating H_2CO in $(\text{HF})_n$ rings breaks the C_{nh} symmetry and, hence, lifts the degeneracies and the strict infrared intensity relations. The

calculated red shifts for the HF stretching vibrations in $\text{H}_2\text{CO}\cdots(\text{HF})_{2\leq n\leq 4}$ clusters collected in Tables 3 and 4 exhibit the patterns encountered in the pure $(\text{HF})_n$ rings. Quantitative differences occur only due to the breakdown of the C_{nh} symmetry and the fact that the HF molecule hydrogen bonded to the C=O group shows even stronger red shifts because of the stronger F–H \cdots O hydrogen bond.

The total stabilization energies, taken without the CP correction, relative to isolated HF monomers, ΔE_b , amount to -13.5 , -28.8 , and $-39.6\text{ kcal mol}^{-1}$ for the cyclic series $(\text{HF})_3$ to $(\text{HF})_5$. The corresponding energies for the series of cyclic $\text{H}_2\text{CO}\cdots(\text{HF})_{2\leq n\leq 4}$ complexes are -18.5 , -28.4 , and $-37.6\text{ kcal mol}^{-1}$, respectively (see Table 2). Redefining the stabilization energy relative to the HF monomer and the $(\text{HF})_{n-1}$ cluster yields ΔE_a equal to -7.5 , -10.7 , and $-8.8\text{ kcal mol}^{-1}$ for the series $(\text{HF})_3$ to $(\text{HF})_5$, which may be confronted with the ΔE_a values of -13.8 , -13.0 , and $-8.6\text{ kcal mol}^{-1}$ for the $\text{H}_2\text{CO}\cdots(\text{HF})_{2\leq n\leq 4}$ series given in Table 2.

5. Summary and Conclusions

In this work, we have presented the results of large-scale ab initio calculations of the structures and vibrational spectra of the hitherto unobserved cyclic $\text{H}_2\text{CO}\cdots(\text{HF})_{1\leq n\leq 4}$ clusters which are primarily stabilized by strong F–H \cdots O=C and F–H \cdots F hydrogen bonds. The C–H \cdots F hydrogen bonds in the clusters $\text{H}_2\text{CO}\cdots(\text{HF})_{2\leq n\leq 4}$ constitute the weakest intermolecular contacts. Whereas all the F–H stretching modes are significantly red-shifted, in accordance with the conventional picture of hydrogen bonding, we have computationally predicted unusually large blue shifts of the C–H stretching modes, exceeding 100 cm^{-1} . As the number of hydrogen fluoride molecules in the ring grows, the blue shifts of the C–H stretching modes increase. What is the origin of such unexpectedly large blue shifts of these modes which are comparable, by the absolute value, with the well-known red shift of the archetypical conventional hydrogen-bonded water dimer system?

We have inferred that the predicted large blue shifts are not merely a direct consequence of the formation of C–H \cdots F hydrogen bonds. Rather, on the contrary, it is to a considerable degree the strong F–H \cdots O=C hydrogen bond formed between the carbonyl group of formaldehyde and the hydrogen fluoride oligomer that, through intramolecular coupling, causes a contraction of the C–H bonds, no matter whether the latter are involved in C–H \cdots F hydrogen bonds or not. This conclusion is obviously irrefutable for the $\text{H}_2\text{CO}\cdots\text{HF}$ dimer, which does not have a C–H \cdots F hydrogen bond, but nevertheless the symmetric and asymmetric C–H stretches, however, undergo rather large blue shifts of 44 and 68 cm^{-1} .

In this regard, we may recall that the very same conclusion on the predominant role of the intramolecular coupling for the blue shifts of the C–H stretches has also been drawn for the complexes of fluoromethanes^{9,10} and fluorosilanes¹¹ with hydrogen fluoride clusters for which the term *blue-shifted* has been thus introduced. It is therefore to be expected that intramolecular couplings also play an important role in other cyclic complexes with blue-shifted hydrogen bonds.

Acknowledgment. The calculations were performed on the Linux-cluster Schrödinger II at the University of Vienna. The authors are grateful for ample supply of computer time at this installation. One of the authors, E.S.K., thanks Françoise Remacle for warm hospitality and the F.R.F.C. 2.4562.03F (Belgium) for a fellowship. We also thank a reviewer for valuable suggestions and comments.

References and Notes

- (1) Desiraju, G. R.; Steiner, T. *The Weak Hydrogen Bond in Structural Chemistry and Biology*; Oxford University Press: New York, 1999.
- (2) Allerhand, A.; Schleyer, P. v. R. *J. Am. Chem. Soc.* **1963**, *85*, 1715.
- (3) Green, R. D. *Hydrogen Bonding by C-H Groups*; MacMillan: London, UK, 1974.
- (4) (a) Hartmann, M.; Wetmore, S. D.; Radom, L. *J. Phys. Chem. A* **2001**, *105*, 4470. (b) Scheiner, S.; Grabowski, S. J.; Kar, T. *J. Phys. Chem. A* **2001**, *105*, 10607.
- (5) Pimentel, C. G.; McClellan, A. L. *The Hydrogen Bond*; W. H. Freeman: San Francisco, CA, 1960.
- (6) Schuster, P.; Zundel, G. C.; Sandorfy, C., Eds. *The Hydrogen Bond. Recent Developments in Theory and Experiments*; North-Holland: Amsterdam, The Netherlands, 1976.
- (7) Scheiner, S. *Hydrogen Bonding: A Theoretical Perspective*; Oxford University Press: New York, 1997.
- (8) Barnes, A. J. *J. Mol. Struct.* **2004**, *704*, 3.
- (9) Karpfen, A.; Kryachko, E. S. *J. Phys. Chem. A* **2003**, *107*, 9724.
- (10) Karpfen, A.; Kryachko, E. S. *Chem. Phys.* **2005**, *309*, 000.
- (11) Karpfen, A. *J. Mol. Struct. (THEOCHEM)* **2004**, *710*, 85.
- (12) Baiocchi, F. A.; Klemperer, W. *J. Chem. Phys.* **1983**, *78*, 3509.
- (13) Lovas, F. J.; Suenram, R. D.; Ross, S.; Klubowski, M. *J. Mol. Spectrosc.* **1987**, *123*, 167.
- (14) Magnasco, V.; Costa, C.; Figari, G. *Chem. Phys. Lett.* **1989**, *160*, 469.
- (15) Platts, J. A.; Howard, S. T.; Bracke, B. R. F. *J. Am. Chem. Soc.* **1996**, *118*, 2726.
- (16) Bobadova-Parvanova, P.; Galabov, B. *J. Phys. Chem. A* **1998**, *102*, 1815.
- (17) Gadre, S. R.; Bhadane, P. K. *J. Phys. Chem. A* **1999**, *103*, 3512.
- (18) Galabov, B.; Bobadova-Parvanova, P. *J. Phys. Chem. A* **1999**, *103*, 6793.
- (19) Salai Cheettu Ammal, S.; Venuvanalingam, P. *J. Phys. Chem. A* **2000**, *104*, 10859.
- (20) (a) Wisniewska, M.; Grabowski, S. *J. Monatsh. Chem.* **2002**, *133*, 305. (b) Grabowski, S. *J. J. Phys. Org. Chem.* **2004**, *17*, 18. (c) Li, R. Y.; Li, Z. R.; Wu, D.; Hao, X. Y.; Li, R. J.; Sun, C. C. *Int. J. Quantum Chem.* **2005**, *103*, 157.
- (21) Möller, C.; Plesset, M. S. *Phys. Rev.* **1934**, *46*, 618.
- (22) Frisch, M. J.; Trucks, G. W.; Schlegel, H. B.; Scuseria, G. E.; Robb, M. A.; Cheeseman, J. R.; Zakrzewski, V. G.; Montgomery, J. A.; Stratmann, R. E.; Burant, J. C.; Dapprich, S.; Millan, J. M.; Daniels, A. D.; Kudin, K. N.; Strain, M. C.; Farkas, O.; Tomasi, J.; Barone, V.; Cossi, M.; Cammi, R.; Mennucci, B.; Pomelli, C.; Adamo, C.; Clifford, S.; Ochterski, J.; Peterson, G. A.; Ayala, P. Y.; Cui, Q.; Morokuma, K.; Malick, D. K.; Rabuck, A. D.; Raghavachari, K.; Foresman, J. B.; Cioslowski, J.; Ortiz, J. V.; Stefanov, B. B.; Liu, G.; Liashenko, A.; Piskorz, P.; Komaromi, I.; Gomperts, R.; Martin, R. L.; Fox, D. J.; Keith, T.; Al-Laham, M. A.; Peng, C. Y.; Nanayakkara, A.; Gonzalez, C.; Challacombe, M.; Gill, P. M. W.; Johnson, B. G.; Chen, W.; Wong, M. W.; Andres, J. L.; Head-Gordon, M.; Replogle, E. S.; Pople, J. A. *GAUSSIAN 98*; Gaussian, Inc.: Pittsburgh, PA, 1998.
- (23) Gordon, M. S.; Binkley, J. S.; Pople, J. A.; Pietro, W. J.; Hehre, W. J. *J. Am. Chem. Soc.* **1982**, *104*, 2797.
- (24) Francl, M. M.; Pietro, W. J.; Hehre, W. J.; Binkley, J. S.; Gordon, M. S.; Defrees, D. J.; Pople, J. A. *J. Chem. Phys.* **1982**, *77*, 3654.
- (25) McLean, A. D.; Chandler, G. S. *J. Chem. Phys.* **1980**, *72*, 5639.
- (26) Frisch, M. J.; Pople, J. A.; Binkley, J. S. *J. Chem. Phys.* **1984**, *80*, 3265.
- (27) Krishnan, R.; Binkley, J. S.; Seeger, R.; Pople, J. A. *J. Chem. Phys.* **1980**, *72*, 650.
- (28) Clark, T.; Chandrasekhar, J.; Spitznagel, G. W.; Schleyer, P. v. R. *J. Comput. Chem.* **1983**, *4*, 294.
- (29) Woon, D. E.; Dunning, T. H., Jr. *J. Chem. Phys.* **1993**, *98*, 1358.
- (30) Kendall, R. E.; Dunning, T. H., Jr.; Harrison, R. J. *J. Chem. Phys.* **1992**, *96*, 6796.
- (31) Boys, S. F.; Bernardi, F. *Mol. Phys.* **1970**, *19*, 553.
- (32) Karpfen, A. *Int. J. Quantum Chem. Quantum. Chem. Symp.* **1990**, *24*, 129.
- (33) Latajka, Z.; Scheiner, S. *Chem. Phys.* **1988**, *122*, 413.
- (34) Karpfen, A. *Adv. Chem. Phys.* **2002**, *123*, 469.
- (35) Klopper, W.; Quack, M.; Suhm, M. A. *Mol. Phys.* **1998**, *94*, 105.
- (36) (a) Morokuma, K. *J. Chem. Phys.* **1971**, *55*, 1236. (b) Del Bene, J. E. *J. Chem. Phys.* **1975**, *62*, 1314. (c) Ramelot, T. A.; Hu, C.-H.; Fowler, J. E.; DeLeeuw, B. J.; Schaefer, H. F., III. *J. Chem. Phys.* **1994**, *100*, 4347.
- (37) Murray-Rust, P.; Glusker, J. P. *J. Am. Chem. Soc.* **1984**, *106*, 1018.
- (38) This study on the formaldehyde-water complex by Schaefer and co-workers^{36c} also reveals that the shortest distance between the water oxygen and a hydrogen of formaldehyde is equal to 2.701 Å (with the $\angle\text{C}-\text{H}\cdots\text{O} = 104.0^\circ$). In this regard, the authors^{36c} conclude that, in contrast with the interpretation by Kumpf and Damewood (Kumpf, R. A.; Damewood, J. R., Jr. *J. Phys. Chem.* **1989**, *93*, 4478) of such complex as “ring-like”, there exists “little evidence” of the interaction between the water oxygen and this formaldehyde hydrogen. A similar statement about a “ring-like” structure of formaldehyde-HF complex and formation of a blue-shifting hydrogen bond between F and a hydrogen of H₂CO has recently been made by Li et al.,^{20c} who report the distance $r(\text{H}\cdots\text{F}) = 2.984 \text{ \AA}$ (MP2/6-311++G(3df, 3pd)) that is larger than the sum of van der Waals radii of H and F (a so-called van der Waals cutoff condition for conventional hydrogen bonds). Li et al.^{20c} has also demonstrated that this hydrogen bonding interaction causes a blue shift of the $\nu(\text{C}-\text{H})$ of formaldehyde by 70 cm^{-1} and a contraction of the corresponding C-H bond by 0.003 \AA .
- (39) Dimitrova, Y. *Spectrochim. Acta Part A* **1998**, *54*, 629.
- (40) (a) Ford, G. P.; Scribner, J. D. *J. Comput. Chem.* **1983**, *4*, 594. (b) Olivella, S.; Urpi, F.; Vilarrasa, J. *J. Comput. Chem.* **1984**, *5*, 230. (c) Del Bene, J. E. *J. Comput. Chem.* **1985**, *6*, 296. (d) Dewar, M. J. S.; Dieter, K. M. *J. Am. Chem. Soc.* **1986**, *108*, 8075. (e) Ozment, J. L.; Schmiedekamp, A. M. *Int. J. Quantum Chem.* **1992**, *43*, 783. (f) Hartz, N.; Rasul, G.; Olah, G. J. *Am. Chem. Soc.* **1993**, *115*, 1277. (g) Smith, B. J.; Radom, L. *J. Am. Chem. Soc.* **1993**, *115*, 4885. (h) Smith, B. J.; Radom, L. *Chem. Phys. Lett.* **1994**, *231*, 345. (i) Speers, P.; Laidig, K. E. *J. Chem. Soc., Perkin Trans. 2* **1994**, 799. (j) Badenhoop, J. K.; Scheiner, S. *J. Chem. Phys.* **1996**, *105*, 4675. (k) Del Bene, J. E.; Gwaltney, S. R.; Bartlett, R. J. *J. Phys. Chem. A* **1998**, *102*, 5124. (l) Grana, A. M.; Mosquera, R. A. *Chem. Phys.* **1999**, *243*, 17. (m) Chandra, A. K.; Nguyen, M. T.; Zeegers-Huyskens, T. *Chem. Phys.* **2000**, *255*, 149. (n) Del Bene, J. E.; Watts, J. D. *Int. J. Quantum Chem.* **2000**, *77*, 187. (o) Antol, I.; Eckert-Maksia, M.; Müller, T.; Dallos, M.; Lischka, H. *Chem. Phys. Lett.* **2003**, *374*, 587.
- (41) (a) Takagi, K.; Oka, T. *J. Phys. Soc. Jpn.* **1963**, *18*, 1174. (b) Dore, L.; Cazzoli, G.; Civiš, S.; Scapini, F. *J. Mol. Spectrosc.* **1997**, *183*, 107. (c) See also: *NIST Chemistry WebBook*, NIST Standard Reference Database Number 69; Linstrom, P. J., Mallard, W. G., Eds.; National Institute of Standards and Technology: Gaithersburg, MD, 2001, pp 20899, <http://webbook.nist.gov>.
- (42) (a) Lias, S. G.; Liebman, J. F.; Levin, R. D. *J. Phys. Chem. Ref. Data* **1984**, *13*, 695. (b) Hunter, E. P.; Lias, S. G. *J. Phys. Chem. Ref. Data* **1998**, *27*, 413.
- (43) (a) Wiberg, K. M.; Laidig, K. E. *J. Am. Chem. Soc.* **1987**, *109*, 5935. (b) Wiberg, K. B.; Marquez, M.; Castejon, H. *J. Org. Chem.* **1994**, *59*, 6817. (c) Reference 40i. (d) Wiberg, K. B. *Acc. Chem. Res.* **1999**, *32*, 922.
- (44) Burleigh, D. C.; McCoy, A. B.; Sibert, E. L., III. *J. Chem. Phys.* **1998**, *104*, 480.
- (45) Masunov, A.; Dannenberg, J. J.; Contreras, R. H. *J. Phys. Chem. A* **2001**, *105*, 4737.
- (46) Qian, W.; Krimm, S. *J. Phys. Chem. A* **2002**, *106*, 6628.
- (47) Pejov, L.; Hermansson, K. *J. Chem. Phys.* **2003**, *119*, 313.